Journal of Environment and Engineering

Vol. 3, No. 2, 2008

Hybrid Vibration Suppression of Flexible Structures Using Piezoelectric Elements and Analog Circuits*

Keisuke YAMADA**, Hiroshi MATSUHISA**, Hideo UTSUNO**
and Jeong Gyu PARK***

**Department of Mechanical Engineering and Science, Kyoto University,
Yoshida-Honmachi, Sakyo-ku, Kyoto 606-8501, Japan
E-mail: yamada@me.kyoto-u.ac.jp
***LG Electronics Inc.,
PERI, 19-1 Cheongho-ri, Jinwuy-myun, Pyungtaek-si, Kyunggi-do, 451-713, Korea

Abstract

This paper describes a new hybrid vibration suppression technique for flexible structures like beams and plates using piezoelectric elements and analog circuits. There are two main methods to suppress vibration of flexible structures. One is active vibration control and the other is passive vibration suppression. The former is often effective but has a stability problem. While the latter avoids such instability, its controlling force is small. Hence, this paper is proposing a new hybrid vibration suppression method that is stable and effective. The optimum values of the circuit are determined by simple formulations derived by Two Fixed Points Method. The proposed method is verified by experiments that demonstrate that the hybrid method works better than conventional passive vibration suppression methods.

Key words: Vibration Control, Flexible Structure, Piezoelectric Element, Modal Analysis, Analog Control

1. Introduction

Bending vibration suppression of flexible structures like beams and plates using piezoelectric elements has attracted attention among researchers in recent years. The reasons are that the devices using piezoelectric elements do not require a lot of space compared to mechanical devices like dynamic vibration absorbers and active mass dampers, and controlling force is large. There are two main types of vibration suppression using piezoelectric elements: active vibration control[(1), (2)] and passive vibration suppression[(3)-(6)]. In active control, voltage from a controller is applied to piezoelectric elements to suppress vibration. On the other hand, passive vibration suppression only involves electrical inductances, resistances, and sometimes capacitances coupled to piezoelectric elements, and they work as a vibration absorber. Both of them have drawback and advantage, and those problems have been tackled and solved for the last few decades. For instance, a self-sensing piezoelectric actuator was proposed to realize collocation of a sensor and an actuator for active vibration control[(2)], and a passive method which can suppress multiple vibration modes was proposed by using a multiple degrees of freedom circuit[(6)].

It is well known that the controlling force in active vibration control can be large compared to a passive method, but such controls pose a stability problem. On the contrary, systems do not become unstable in passive vibration suppression, but the controlling force

*Received 16 July, 2008 (No. T1-05-0284)
Japanese Original : Trans. Jpn. Soc. Mech. Eng., Vol.72, No.716, C (2006), pp.1145-1153 (Received 17 Mar, 2005)
[DOI: 10.1299/jee.3.424]

is not as large as that of the active control. Hence, several hybrid vibration suppression methods have also been studied in recent years[7]-[9]. Most of them increase stability of active vibration control by installing a passive method. Those studies turn out that not only stability of the system is improved but also electrical power consumption of active vibration control part can be reduced by the hybridization. However, those hybrid methods simply involve both an active vibration control device and passive vibration suppression one, and as a consequence, the whole device becomes large and the problem of each method is not inherently solved. In order to solve this problem, a new hybrid vibration suppression method based on mechanism of passive vibration suppression is proposed in this paper. The proposed hybrid method does not require any digital controllers, and only an electrical circuit which consists of an inductance, a resistance, and an amplifier has to be tuned optimally. The effectiveness of the proposed method is validated by simulated results and experimental ones.

2. Theoretical Analysis

2.1 Governing Equations

A model of the proposed hybrid vibration suppression method is shown in Fig. 1. This model consists of a plate as a vibration suppression target, two groups of piezoelectric elements, and an electrical circuit. Two groups of piezoelectric elements are used for passive and active methods, respectively. Piezoelectric elements attached to the upper side of the plate are used for passive vibration suppression, and ones on the under side of the plate are for active vibration suppression in Fig. 1. The actuator and sensor equations are given as follows.

$$\boldsymbol{M}\ddot{\boldsymbol{\xi}} + \boldsymbol{K}\boldsymbol{\xi} - \boldsymbol{\Theta}_{\mathrm{P}} v_{\mathrm{Pa}} - \boldsymbol{\Theta}_{\mathrm{A}} v_{\mathrm{Aa}} = \boldsymbol{Q} P_{\mathrm{f}}, \tag{1}$$

$$\boldsymbol{\Theta}_{\mathrm{P}}^{\mathrm{t}} \boldsymbol{\xi} + C_{\mathrm{pP}}^{\mathrm{S}} v_{\mathrm{Ps}} = q_{\mathrm{P}}, \tag{2}$$

$$\boldsymbol{\Theta}_{\mathrm{A}}^{\mathrm{t}} \boldsymbol{\xi} + C_{\mathrm{pA}}^{\mathrm{S}} v_{\mathrm{As}} = q_{\mathrm{A}}, \tag{3}$$

where $\boldsymbol{M}$ is a modal mass matrix, $\boldsymbol{K}$ is a modal stiffness matrix, $\boldsymbol{\Theta}$ is a modal electromechanical coupling coefficients matrix, $\boldsymbol{Q}$ is a modal influence matrix of external force, C_{p} is a combined capacitance of a group of piezoelectric elements, $\boldsymbol{\xi}$ is a modal displacement vector of the plate, v is voltage between the electrodes of the combined piezoelectric elements, P_{f} is an external uniformly-distributed force, and q is charge in a combined piezoelectric element. The superscript t denotes conventional matrix transpose, the superscript S denotes the boundary condition under which the strain is constant, the subscripts P and A denote combined piezoelectric elements for passive and active vibration suppression, respectively, and the subscripts a and s denote applied and sensed voltages, respectively. Here it is assumed that there is no stress transmission between two groups of piezoelectric elements in Eqs. (2) and (3). Practically the stress generated by each group of piezoelectric elements partially transmits to the other group of piezoelectric element; however, it is impossible to derive its fraction theoretically because it depends on material property and thickness of the plate, relationship between locations of two groups of piezoelectric elements, condition of the adhesive, and so on, and the transmitted stress is sometimes small enough to be ignored. In the following theoretical analysis, the capacitance $C_{\mathrm{pP}}^{\mathrm{S}}$

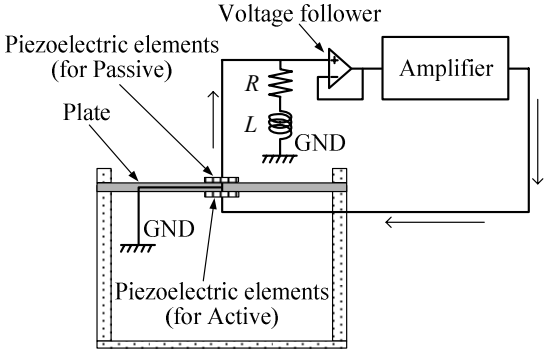

Fig. 1 Model of hybrid vibration suppression.

derived by ignoring the stress transmission is used; however, the way to compensate the change of capacitance when stress transmission can not be ignored is hereinafter described.

As shown in Fig. 1, the combined piezoelectric element for passive vibration suppression is coupled to a LR circuit. Both piezoelectric effect and inverse piezoelectric effect are used in passive vibration suppression. From Eq. (2), the sensed voltage in the combined piezoelectric element for passive vibration suppression is derived as

$$v_{\mathrm{Ps}} = -\frac{\boldsymbol{\Theta}_{\mathrm{P}}^{\mathrm{t}}}{C_{\mathrm{pP}}^{\mathrm{S}}}\boldsymbol{\xi} + \frac{q_{\mathrm{P}}}{C_{\mathrm{pP}}^{\mathrm{S}}}. \tag{4}$$

The circuit equation of the electrical system composed of a LR circuit and a combined piezoelectric element for passive vibration suppression is defined as

$$v_{\mathrm{z}} + v_{\mathrm{Ps}} = 0, \tag{5}$$

where v_{z} is voltage of the LR circuit and given by

$$v_{\mathrm{z}} = \begin{cases} L\ddot{q}_{\mathrm{P}} + R\dot{q}_{\mathrm{P}} & (\text{series LR circuit}) \\ \dfrac{j\omega LR}{j\omega L + R}\dot{q}_{\mathrm{P}} & (\text{parallel LR circuit}) \end{cases}. \tag{6}$$

Here L and R are an inductance and a resistance of the LR circuit, respectively, and ω is a frequency of the external force. While a series LR circuit is used in Fig. 1, a parallel LR circuit can also be used instead of the series type. The voltage applied to the combined piezoelectric element for passive vibration suppression is identical with the back electromotive force generated by the LR circuit.

$$v_{\mathrm{Pa}} = -v_{\mathrm{z}}. \tag{7}$$

Because both the applied voltage v_{Pa} and the sensed voltage v_{Ps} are the voltage between the electrodes of the combined piezoelectric element, they are equal.

$$v_{\mathrm{Pa}} = v_{\mathrm{Ps}}. \tag{8}$$

Since only inverse piezoelectric effect is used in the active vibration supperssion part of the proposed method, the sensed voltage v_{As} given by Eq. (3) is not necessary. In the electrical circuit, the voltage v_{Pa} which is the applied voltage to the combined piezoelectric element for passive vibration suppression is pulled out by a voltage follower, and the voltage is amplified by an amplifier, and finally the amplified voltage is applied to the combined piezoelectric element for active vibration suppression. The applied voltage v_{Aa} is defined as

$$v_{\mathrm{Aa}} = \alpha v_{\mathrm{Pa}}, \tag{9}$$

where α is an amplification factor of the amplifier. Substituting Eqs. (7) and (9) into Eq. (1) gives

$$\boldsymbol{M}\ddot{\boldsymbol{\xi}} + \boldsymbol{K}\boldsymbol{\xi} + \left(\boldsymbol{\Theta}_{\mathrm{P}} + \alpha\boldsymbol{\Theta}_{\mathrm{A}}\right)v_{\mathrm{z}} = \boldsymbol{Q}P_{\mathrm{f}}. \tag{10}$$

Equations (5) and (10) are the governing equations of the model shown in Fig. 1. The LR circuit works as not only a vibration suppression device for passive vibration suppression part but also a control signal generator for active vibration suppression part in this method. As a consequence, this method requires neither a sensor nor an external controller additionally.

2.2 Compliance

Because the proposed method can suppress only a single vibration mode and the performance is evaluated by the amplitude of the resonance peak, only the target vibration mode is employed and the governing Eqs. (5) and (10) can be written as follows.

$$M_{\mathrm{i}}\ddot{\xi}_{\mathrm{i}} + K_{\mathrm{i}}\xi_{\mathrm{i}} + \left(1 + \kappa_{\mathrm{i}}\alpha\right)\Theta_{\mathrm{Pi}}v_{\mathrm{z}} = Q_{\mathrm{i}}P_{\mathrm{f}}, \tag{11}$$

$$v_{\mathrm{z}} + \frac{q_{\mathrm{P}}}{C_{\mathrm{pP}}^{\mathrm{S}}} = \frac{\Theta_{\mathrm{Pi}}}{C_{\mathrm{pP}}^{\mathrm{S}}}\xi_{\mathrm{i}}, \tag{12}$$

$$\kappa_{\mathrm{i}} = \frac{\Theta_{\mathrm{Ai}}}{\Theta_{\mathrm{Pi}}}. \tag{13}$$

Here i denotes the targeted vibration mode. From Eqs. (11) and (12), nondimensional compliance can be derived as

$$\frac{\xi_{\mathrm{i}}}{\xi_{\mathrm{sti}}} = \frac{1}{-g_{\mathrm{i}}^2 + 1 + \beta_{\mathrm{Pi}}\left(1+\kappa_{\mathrm{i}}\alpha\right)G_{\mathrm{Hi}}}, \tag{14}$$

$$G_{\mathrm{Hi}} = \begin{cases} \dfrac{-g_{\mathrm{i}}^2 + 2j\zeta_{\mathrm{i}} f_{\mathrm{i}} g_{\mathrm{i}}}{f_{\mathrm{i}}^2 - g_{\mathrm{i}}^2 + 2j\zeta_{\mathrm{i}} f_{\mathrm{i}} g_{\mathrm{i}}} & \left(\text{series LR circuit}\right) \\ \dfrac{-g_{\mathrm{i}}^2}{f_{\mathrm{i}}^2 - g_{\mathrm{i}}^2 + 2j\zeta_{\mathrm{i}} f_{\mathrm{i}} g_{\mathrm{i}}} & \left(\text{parallel LR circuit}\right) \end{cases}, \tag{15}$$

$$\xi_{\mathrm{sti}} = \frac{Q_{\mathrm{i}} P_{\mathrm{f}}}{K_{\mathrm{i}}},\quad g_{\mathrm{i}} = \frac{\omega}{\Omega_{\mathrm{i}}},\quad \Omega_{\mathrm{i}} = \sqrt{\frac{K_{\mathrm{i}}}{M_{\mathrm{i}}}},$$

$$\beta_{\mathrm{Pi}} = \frac{\Theta_{\mathrm{Pi}}^2}{K_{\mathrm{i}} C_{\mathrm{pP}}^{\mathrm{S}}},\quad f_{\mathrm{i}} = \frac{\omega_{\mathrm{ai}}}{\Omega_{\mathrm{i}}},\quad \omega_{\mathrm{ai}} = \sqrt{\frac{1}{L_{\mathrm{i}} C_{\mathrm{pP}}^{\mathrm{S}}}},$$

$$\zeta_{\mathrm{i}} = \begin{cases} \dfrac{R_{\mathrm{i}}}{2}\sqrt{\dfrac{C_{\mathrm{pP}}^{\mathrm{S}}}{L_{\mathrm{i}}}} & \left(\text{series LR circuit}\right) \\ \dfrac{1}{2R_{\mathrm{i}}}\sqrt{\dfrac{L_{\mathrm{i}}}{C_{\mathrm{pP}}^{\mathrm{S}}}} & \left(\text{parallel LR circuit}\right) \end{cases}.$$

From Eq. (14), magnitude of the nondimensional compliance is given as

$$u_{\mathrm{Ci}} = \left|\frac{\xi_{\mathrm{i}}}{\xi_{\mathrm{sti}}}\right| = \sqrt{\frac{A_{\mathrm{i}}^2 + 4\zeta_{\mathrm{i}}^2 B_{\mathrm{i}}^2}{E_{\mathrm{i}}^2 + 4\zeta_{\mathrm{i}}^2 F_{\mathrm{i}}^2}}, \tag{16}$$

$$A_{\mathrm{i}} = f_{\mathrm{i}}^2 - g_{\mathrm{i}}^2,\quad B_{\mathrm{i}} = f_{\mathrm{i}} g_{\mathrm{i}},\quad E_{\mathrm{i}} = \left(1-g_{\mathrm{i}}^2\right)\left(f_{\mathrm{i}}^2 - g_{\mathrm{i}}^2\right) - \beta_{\mathrm{Pi}}\left(1+\kappa_{\mathrm{i}}\alpha\right)g_{\mathrm{i}}^2,$$

$$F_{\mathrm{i}} = \begin{cases} f_{\mathrm{i}} g_{\mathrm{i}}\left[1 + \beta_{\mathrm{Pi}}\left(1+\kappa_{\mathrm{i}}\alpha\right) - g_{\mathrm{i}}^2\right] & \left(\text{series LR circuit}\right) \\ f_{\mathrm{i}} g_{\mathrm{i}}\left(1-g_{\mathrm{i}}^2\right) & \left(\text{parallel LR circuit}\right) \end{cases}.$$

Because the vibration suppression mechanism of the proposed hybrid method is based on the passive vibration suppression, Eq. (16) is similar to that of the passive vibration suppression using a LR circuit[3].

The performance of passive vibration suppression is determined by an equivalent stiffness ratio β. Values of the LR circuit elements have no relationship to the performance but must be tuned optimally. The performance of the proposed hybrid method can arbitrarily be tuned by α and κ_{i} because β_{Pi} which is the equivalent stiffness ratio of the combined piezoelectric element for passive vibration suppression is multiplied by $\left(1+\kappa_{\mathrm{i}}\alpha\right)$ as shown in Eq. (14).

2.3 Optimum Tuning of a LR Circuit by Use of Two Fixed Points Method

Optimum values of the LR circuit elements are formulated by use of Two Fixed Points Method[10]. Two Fixed Points Method is a popular method for finding the optimum natural frequency ratio and the optimum damping ratio of the additional single degree of freedom system such as a dynamic vibration absorber. This method can also be applied to the optimum tuning of the LR circuit in the proposed hybrid method.

The frequency response of Eq. (16) has two fixed points regardless of the value of the damping ratio ζ_{i}. The optimum natural frequency ratio f_{opti} is determined as the amplitudes at the two fixed points are equal, and the optimum damping ratio ζ_{opti} is derived so that the amplitudes become maximum at the two fixed points.

The optimum natural frequency ratio f_{opti} is derived on condition that the amplitudes at the two fixed points P and Q are equal.

$$f_{\mathrm{opti}}=\begin{cases}\sqrt{1+\beta_{\mathrm{Hi}}} & (\text{series LR circuit})\\ \sqrt{\dfrac{2-\beta_{\mathrm{Hi}}}{2}} & (\text{parallel LR circuit})\end{cases}, \tag{17}$$

$$\beta_{\mathrm{Hi}}=\beta_{\mathrm{Pi}}\left(1+\kappa_{\mathrm{i}}\alpha\right)=\frac{\Theta_{\mathrm{Pi}}^{2}}{K_{\mathrm{i}}C_{\mathrm{pP}}^{\mathrm{S}}}\left(1+\kappa_{\mathrm{i}}\alpha\right). \tag{18}$$

From Eqs. (16) and (17), the nondimensional frequency ratios at the two fixed points are given as

$$g_{\mathrm{P,Qi}}=\begin{cases}\sqrt{\left(1+\beta_{\mathrm{Hi}}\right)\mp\sqrt{\dfrac{\beta_{\mathrm{Hi}}\left(1+\beta_{\mathrm{Hi}}\right)}{2}}} & (\text{series LR circuit})\\ \sqrt{1\mp\sqrt{\dfrac{\beta_{\mathrm{Hi}}}{2}}} & (\text{parallel LR circuit})\end{cases}. \tag{19}$$

The amplitudes at the two fixed points are derived as follows.

$$u_{\mathrm{Ci}}\Big|_{g_{\mathrm{i}}=g_{\mathrm{P,Qi}}}=\begin{cases}\sqrt{\dfrac{2}{\beta_{\mathrm{Hi}}\left(1+\beta_{\mathrm{Hi}}\right)}} & (\text{series LR circuit})\\ \sqrt{\dfrac{2}{\beta_{\mathrm{Hi}}}} & (\text{parallel LR circuit})\end{cases}. \tag{20}$$

The damping ratios which make the amplitudes at P and Q maximum are not equal; however, the difference is small enough to be ignored. Then the optimum damping ratio ζ_{opti} is approximately given by their average.

$$\zeta_{\mathrm{opti}}=\frac{1}{2}\left(\zeta_{\mathrm{Popti}}+\zeta_{\mathrm{Qopti}}\right), \tag{21}$$

$$\zeta_{\mathrm{P,Qopti}}=\frac{1}{2}\sqrt{\frac{-A_{\mathrm{i}}A_{\mathrm{i}}'+u_{\mathrm{Ci}}^{2}E_{\mathrm{i}}E_{\mathrm{i}}'}{B_{\mathrm{i}}B_{\mathrm{i}}'-u_{\mathrm{Ci}}^{2}F_{\mathrm{i}}F_{\mathrm{i}}'}}\Bigg|_{g_{\mathrm{i}}=g_{\mathrm{P,Qi}}}},$$

where $'$ means $\partial/\partial g_{\mathrm{i}}$.

From the optimum natural frequency ratio f_{opti} and the optimum damping ratio ζ_{opti}, optimum values of the inductance and the resistance are formulated as

$$L_{\mathrm{opti}}=\frac{1}{f_{\mathrm{opti}}^{2}}\frac{1}{C_{\mathrm{pP}}^{\mathrm{S}}}\frac{1}{\Omega_{\mathrm{i}}^{2}}, \tag{22}$$

$$R_{\mathrm{opti}}=\begin{cases}2\zeta_{\mathrm{opti}}\dfrac{1}{f_{\mathrm{opti}}}\dfrac{1}{C_{\mathrm{pP}}^{\mathrm{S}}}\dfrac{1}{\Omega_{\mathrm{i}}} & (\text{series LR circuit})\\ \dfrac{1}{2\zeta_{\mathrm{opti}}}\dfrac{1}{f_{\mathrm{opti}}}\dfrac{1}{C_{\mathrm{pP}}^{\mathrm{S}}}\dfrac{1}{\Omega_{\mathrm{i}}} & (\text{parallel LR circuit})\end{cases}. \tag{23}$$

2.4 Performance of the Proposed Method

The performance of the proposed hybrid vibration suppression method can be evaluated by the amplitudes at the two fixed points because the amplitudes at the two fixed points are almost maximum in the frequency response function. As shown in Eq. (20), the amplitudes at the two fixed points are determined only by the equivalent stiffness ratio β_{Hi}, and the vibration decreases as β_{Hi} increases. As the performance of a dynamic vibration absorber is determined by the mass ratio, the performance of the vibration suppression of this study is determined by the stiffness ratio. The robustness is also improved as the value of β_{Hi} becomes large as well as a dynamic vibration absorber. If β_{Hi} is much less than 1, the performances of using series and parallel LR circuits are almost equal, otherwise the performance of using a series LR circuit is better than that of using a parallel LR circuit.

2.5 Transmission of Stress between Two Combined Piezoelectric Elements

If stress transmission between two combined piezoelectric elements is small enough to be ignored, capacitance of the combined piezoelectric element for passive vibration suppression is given by $C_{\mathrm{pP}}^{\mathrm{S}}$. The superscript S denotes the boundary condition under which strain is constant. In this case, β_{Pi} is constant, and β_{Hi} is a linear function of α as expressed in Eq. (18). Meanwhile, if stress transmission between two combined piezoelectric elements can not be ignored, the capacitance of the combined piezoelectric element for passive vibration suppression is not constant because the boundary condition of the constant strain is not satisfied. In this case, the capacitance of the combined piezoelectric element for passive vibration suppression increases in proportion to the strength of the transmitted stress, and it is given as follows.

$$C_{\mathrm{pP}} = C_{\mathrm{pP}}^{\mathrm{S}}\left(1+k_{\alpha}\alpha\right). \tag{24}$$

Here k_{α} is a constant depending on the device, and the sign of k_{α} is equal to that of κ_{i}. C_{pP} given by Eq. (24) must be used in the above-mentioned theoretical analysis instead of $C_{\mathrm{pP}}^{\mathrm{S}}$ if the capacitance of the combined piezoelectric element for passive vibration suppression is varied due to stress transmission. In this case, β_{Hi} is written as

$$\beta_{\mathrm{Hi}} = \beta_{\mathrm{Pi}}\left(1+\kappa_{\mathrm{i}}\alpha\right) = \frac{\Theta_{\mathrm{Pi}}^{2}}{K_{\mathrm{i}}C_{\mathrm{pP}}^{\mathrm{S}}\left(1+k_{\alpha}\alpha\right)}\left(1+\kappa_{\mathrm{i}}\alpha\right). \tag{25}$$

As is evident from Eq. (25), β_{Hi} becomes smaller due to stress transmission.

3. Stability of the System

3.1 Locations of the Two Combined Piezoelectric Elements

Systems of passive vibration suppression using piezoelectric elements are always stable. The primary reason is that there is no external energy supply, and there are several other advantages; a group of piezoelectric elements behaves as both a sensor and an actuator; the controlled voltage is not discrete; and there is no dead time component differently from the active vibration control using a digital controller. Because the hybrid method proposed in this study does not require any external digital controllers, there is no decrease in stability caused by the dead time component and the digital signals. Therefore only the relationship between locations of the combined piezoelectric elements for passive and active vibration suppression can pose instability to the system. Nontarget vibration modes maybe become unstable if the polarity relations of the two combined piezoelectric elements of the vibration modes are different from that of the target vibration mode because of the difference of the mode shapes. In this subsection, the stabilities relevant to nontarget vibration modes are investigated by dividing them into two cases; one is that the polarity relation of the two combined piezoelectric elements is the same as that of the target vibration mode, and the other is that the relation is different.

3.1.1 A Vibration Mode Whose Relation of Polarities is Same

In this case, the signs of κ_{i} and $\kappa_{\mathrm{j}}\left(\mathrm{j}\neq\mathrm{i}\right)$ are same. Here i is a number of the target vibration mode and j is a number of one of the other vibration modes. Nondimensional compliance with respect to jth vibration mode is derived as

$$\frac{\xi_{\mathrm{j}}}{\xi_{\mathrm{st\,j}}} = \frac{1}{-g_{\mathrm{j}}^{2}+1+\beta_{\mathrm{Pj}}\left(1+\kappa_{\mathrm{j}}\alpha\right)G_{\mathrm{Hi\text{-}j}}}, \tag{26}$$

$$G_{\mathrm{Hi\text{-}j}} = \begin{cases} \dfrac{-g_{\mathrm{j}}^{2}+2j\zeta_{\mathrm{i}}f_{\mathrm{i\text{-}j}}g_{\mathrm{j}}}{f_{\mathrm{i\text{-}j}}^{2}-g_{\mathrm{j}}^{2}+2j\zeta_{\mathrm{i}}f_{\mathrm{i\text{-}j}}g_{\mathrm{j}}} & \left(\text{series LR circuit}\right) \\ \dfrac{-g_{\mathrm{j}}^{2}}{f_{\mathrm{i\text{-}j}}^{2}-g_{\mathrm{j}}^{2}+2j\zeta_{\mathrm{i}}f_{\mathrm{i\text{-}j}}g_{\mathrm{j}}} & \left(\text{parallel LR circuit}\right) \end{cases}, \tag{27}$$

$$f_{\text{i-j}} = \frac{\omega_{\text{ai}}}{\Omega_{\text{j}}}.$$

Here $\kappa_{\text{j}}\alpha$ is positive because the signs of κ_{i} and κ_{j} are same. Therefore, if the LR circuit were optimally tuned to suppress jth vibration mode, there would be no essential difference between Eqs. (14) and (26) but the numbers of the target vibration modes. Resonance peak relevant to jth vibration mode is not reduced because the LR circuit is not tuned optimally for jth vibration mode; however, this condition does not destabilize the system. In fact, the system will not be unstable if the relation of polarities is same compared with the target vibration mode. To make all relations of polarities same compared with the target vibration mode, the two combined piezoelectric elements for passive and active vibration suppression must be collocated at the same position of both sides of the target plate.

If the excitation frequency ω is close to the natural frequency of jth vibration mode and the values of Ω_{i} and Ω_{j} are different enough, Eq. (27) is approximately written as follows.

$$G_{\text{Hi-j}} \simeq \begin{cases} 2j\dfrac{\zeta_{\text{i}}}{f_{\text{i-j}}}g_{\text{j}}, & \text{for } \omega \simeq \Omega_{\text{j}} \ll \Omega_{\text{i}} \simeq \omega_{\text{ai}} \\ 1, & \text{for } \omega \simeq \Omega_{\text{j}} \gg \Omega_{\text{i}} \simeq \omega_{\text{ai}} \end{cases}. \tag{28}$$

From Eq. (28), damping or stiffness is increased in a vibration mode whose natural frequency is lower or higher than that of the target vibration mode.

3.1.2 A Vibration Mode Whose Relation of Polarities is Different

Nondimensional compliance relevant to jth vibration mode is the same as Eq. (26); however, $\kappa_{\text{j}}\alpha$ is negative. If $\beta_{\text{P}_{\text{j}}}\left(1+\kappa_{\text{j}}\alpha\right)$ is negative, Eq. (26) can have an unstable pole. From Eq. (27), $G_{\text{Hi-j}}$ is a kind of high pass filters whose cutoff frequency is ω_{ai}. Therefore, vibration modes whose natural frequencies are higher than ω_{ai} are important when the stability is discussed. The stability of the system is determined by the total stiffness of the system and the damping ignored in the theoretical analysis. It is difficult to derive accurately the condition under that the spillover is induced because there are many components. However, the instability of the system is caused by the disagreement of the relation of the polarities. If the damping of the system is high enough, the spillover will not be induced even if the relation of the polarities is different from that of the target vibration mode.

3.2 Methods which Improve Stability

When the amplification factor α is large, the system can be unstable due to the disagreement of the relation of the polarities of the two combined piezoelectric elements at a certain vibration mode. There are two effective methods which avoid such instability of the system in this proposed hybrid method. One method is that of using a low pass filter. This method makes G_{H} small enough to be ignored in a frequency range that is higher than the cutoff frequency of the filter. Since filters induce the change of phase characteristics simultaneously, a suitable filter must be used. The other method is that of using collocation of the two combined piezoelectric elements by use of the upper and under sides of the target. However, it is sometimes difficult to realize the collocation. In this case, the two combined piezoelectric elements should be attached closely because the disagreement of the polarities at a low frequency range can be avoided. Even if spillover might be induced at a high frequency range, an appropriate filter can easily be applied so as to prevent it.

4. Simulation and Experiment

4.1 Experimental Apparatus

A schematic diagram of an experimental apparatus used in this study is shown in Fig. 2. As shown in Fig. 2, the target plate was excited by sound pressure from a speaker. The size of the aluminum plates was $300\text{mm}\times400\text{mm}\times1.0\text{mm}$, and all edges of the plates were clamped. The coordinates of the experimental apparatus are shown in Fig. 3. The z axis is the distance from the neutral plane of the plate. The sound pressure was measured by a microphone located at $(x, y, z)=(0.15\text{m}, 0.10\text{m}, 0.01\text{m})$. The displacement of the plate was measured by an accelerometer located at $(x, y)=(0.15\text{m}, 0.15\text{m})$ on the plate. Nondimensional compliances were derived by using the measured sound pressure and the displacement. As shown in Figs. 4 and 5, two and two, and one and three pieces of piezoelectric elements are attached on the both sides of Plate A and B, respectively. The size of one piece of piezoelectric elements was $22\text{mm}\times32\text{mm}\times0.22\text{mm}$. Piezoelectric elements were connected in parallel, and all of the piezoelectric elements were attached to the plate with conductive adhesives at the center of the plates. The fundamental vibration mode of the plate was suppressed as a target because vibration suppression in a low frequency region is generally important. The natural frequency of the fundamental vibration mode was about 79 Hz. There were also Modes (1,3) and (3,1) in a low frequency region, and their natural frequencies were about 190 Hz and 290 Hz, respectively. The polarity

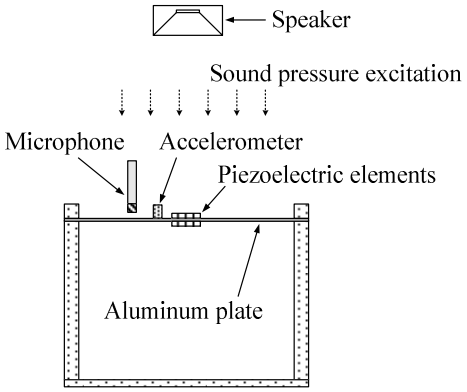

Fig. 2 Schematic diagram of the experimental apparatus.

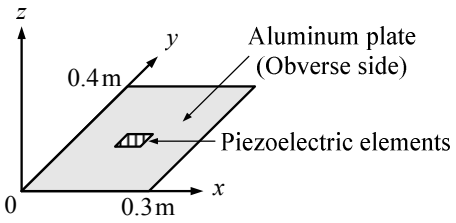

Fig. 3 Coordinates of the plates used in the experiment.

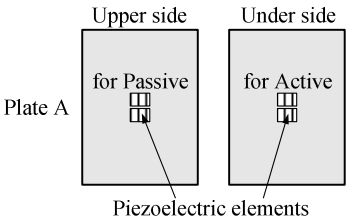

Fig. 4 Schematic diagram of Plate A.

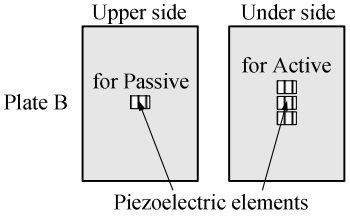

Fig. 5 Schematic diagram of Plate B.

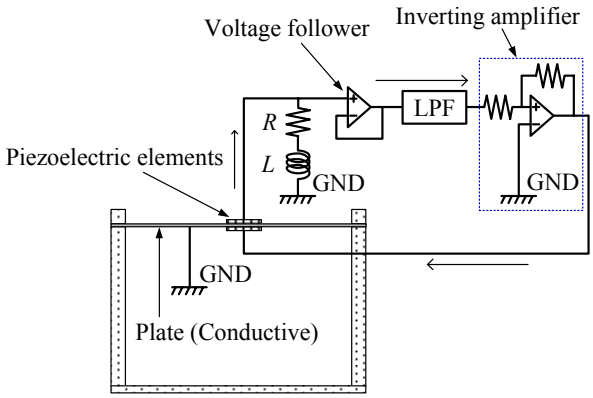

Fig. 6 Detail of the circuit in the experimental apparatus.

relations of the two combined piezoelectric elements at those vibration modes were the same as that of the target vibration mode, and the system with respect to these vibration modes was even stable without a low pass filter. A simulated inductance made by a generalized impedance converter was used because the size of an actual coil was too large and it is troublesome to tune an actual coil. In this experiment, a series LR circuit was used and a low pass filter whose cutoff frequency was 200 Hz was applied to the circuit. The amplification factors were 1, 5, 10, and 20. The spillover was induced when Plate B was excited at $\alpha = 20$ without a low pass filter. A schematic diagram of the circuit used in the experiment is shown in Fig. 6.

4.2 Results of Simulation and Experiment

Material parameters used in the simulation are shown in Table 1. These material parameters were measured in the experiment[11]. The modal damping coefficient D_i of the plate was ignored in the theoretical analysis because vibration suppression is required in low damping structures and theoretical development becomes easy; however, it was included in the simulation because the resonance peak is susceptibly varied by the value of D_i. Simulated and experimental results of the magnitude of the nondimensional compliance are shown in Figs. 7 and 8. The calculated optimum values of the inductance and the resistance are given in Table 2, and the corresponding values in the experiment are shown in Table 3. The values of the equivalent stiffness ratio are also shown in Tables 2 and 3. From the results of the nondimensional compliance and values of the equivalent stiffness ratio, it is shown that the performance of the proposed hybrid method is higher than that of the passive method. However, the experimental results are a little worse than the simulated ones and the difference between the values of the inductances in the simulation and the experiment is large. These disagreements were caused by the change of the capacitance value due to stress transmission between the two combined piezoelectric elements described in § 2.5. The values of C_{pP} measured in the experiment are shown in Table 4. The relationship between α and C_{pP} is also drawn in Fig. 9. The relationship between α and C_{pP} agrees well with Eq. (24). The simulated results of the magnitude of the nondimensional compliance modified by using C_{pP} given in Table 4 are shown in Fig. 10, and the modified calculated optimum values of the series LR circuit and the values of the equivalent stiffness ratio are given in Table 5. These results agree well with the experimental results.

Experimental results of the time response when Plate B was excited randomly by the sound pressure are shown in Fig. 11. The value of the amplification factor in the hybrid method was 20. The proposed hybrid method can suppress only a single vibration mode; however, the difference of the performance can be observed clearly in these time responses.

Table 1 Values of material parameters.

		Plate A		Plate B	
Plate	M_1	1.000	kg	1.000	kg
	K_1	245800	N/m	249800	N/m
	D_1	8.81	Ns/m	14.3	Ns/m
Piezoelectric element (Hybrid)	C_{pP}^S	0.0800	μF	0.0400	μF
	Θ_{P1}	0.00637	N/V	0.00379	N/V
	β_{P1}	0.00206		0.00144	
	κ_1	1.01		2.89	
Piezoelectric element (Passive)	C_p^S	0.0400	μF	0.0300	μF
	Θ_1	0.00617	N/V	0.00514	N/V
	β_1	0.00387		0.00353	

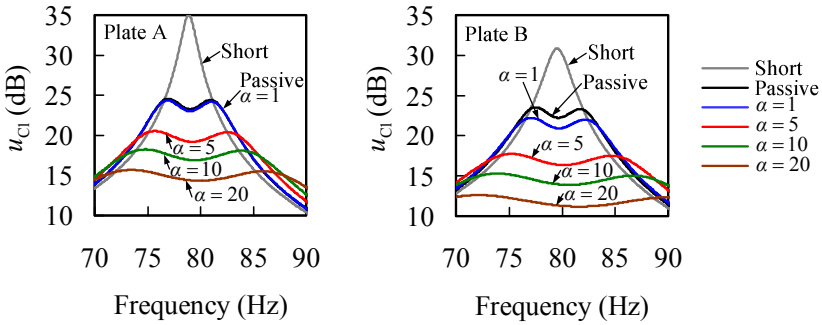

Fig. 7 Simulated results of the compliance with Plate A and B.

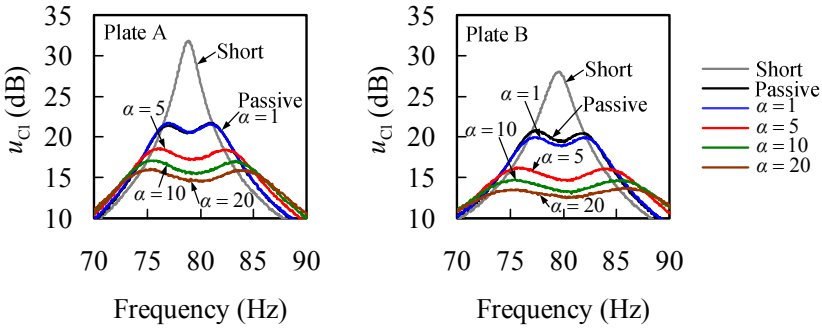

Fig. 8 Experimental results of the compliance with Plate A and B.

Table 2 Calculated optimum values of the series LR circuit and the equivalent stiffness ratios.

		L_{opt1} (H)	R_{opt1} (Ω)	β_1
Plate A	Passive	101	3830	0.00387
	$\alpha = 1$	50.7	1980	0.00414
	$\alpha = 5$	50.2	3410	0.0125
	$\alpha = 10$	49.7	4590	0.0229
	$\alpha = 20$	48.7	6230	0.0437
Plate B	Passive	133	4840	0.00353
	$\alpha = 1$	99.5	4560	0.00560
	$\alpha = 5$	97.9	8970	0.0222
	$\alpha = 10$	95.9	12300	0.0430
	$\alpha = 20$	92.3	16700	0.0846

Table 3 Values of the series LR circuit and the equivalent stiffness ratios in the experiment.

		L_1 (H)	R_1 (Ω)	β_1
Plate A	Passive	90.8	2750	0.00387
	$\alpha = 1$	46.2	1370	0.00389
	$\alpha = 5$	36.9	1840	0.00979
	$\alpha = 10$	29.2	1820	0.0144
	$\alpha = 20$	20.4	853	0.0185
Plate B	Passive	121	3440	0.00353
	$\alpha = 1$	88.8	3180	0.00483
	$\alpha = 5$	68.2	4640	0.0162
	$\alpha = 10$	53.2	4580	0.0245
	$\alpha = 20$	37.1	2720	0.0326

Table 4 Values of C_{pP} at various α.

	Plate A (μF)	Plate B (μF)
$\alpha = 0$	0.0800	0.0400
$\alpha = 1$	0.0881	0.0451
$\alpha = 5$	0.110	0.0587
$\alpha = 10$	0.139	0.0752
$\alpha = 20$	0.199	0.108

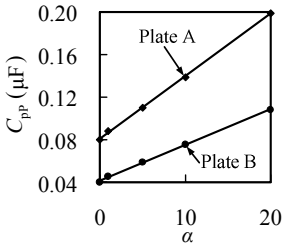

Fig. 9 Relationship between C_{pP} and α.

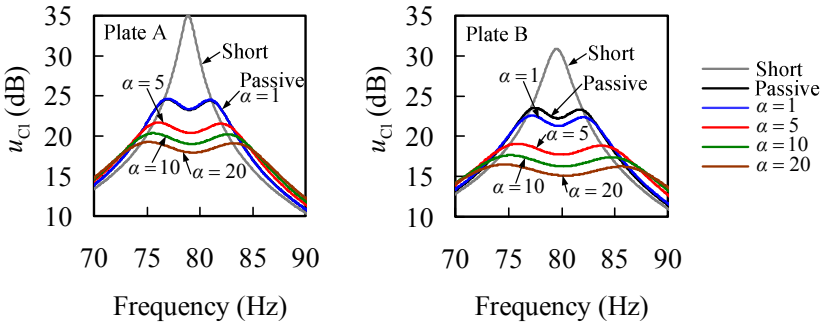

Fig. 10 Modified simulated results of the compliance using C_{pP} shown in Table 4.

Table 5 Modified calculated optimum values of the series LR circuit and the equivalent stiffness ratios.

		L_{opt1} (H)	R_{opt1} (Ω)	β_1
Plate A	Passive	101	3830	0.00387
	$\alpha = 1$	46.0	1710	0.00376
	$\alpha = 5$	36.7	2120	0.00907
	$\alpha = 10$	28.9	2020	0.0132
	$\alpha = 20$	20.1	1620	0.0176
Plate B	Passive	133	4840	0.00353
	$\alpha = 1$	88.3	3810	0.00496
	$\alpha = 5$	67.2	5080	0.0151
	$\alpha = 10$	52.0	4840	0.0229
	$\alpha = 20$	35.9	3920	0.0313

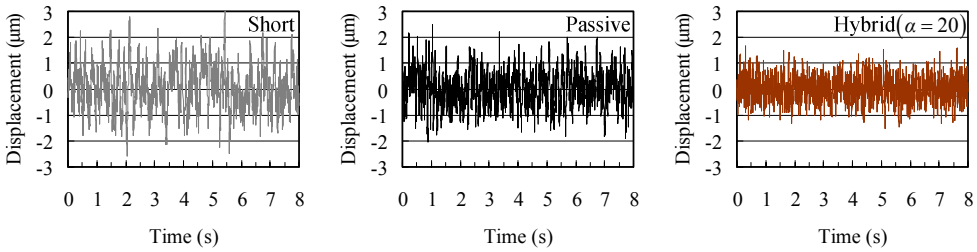

Fig. 11 Random responses using a short circuit, a passive method, and a hybrid method.

5. Conclusion

A new method of hybrid vibration suppression using piezoelectric elements and a LR circuit was proposed. This method is based on passive vibration suppression mechanism

using piezoelectric elements and a LR circuit. The controlling force of a passive method part is amplified by the additional implement in this method. The optimum values of the LR circuit were formulated by use of Two Fixed Points Method. The effectiveness of the proposed method and the theoretical analysis was validated by the simulation and the experiment.

It is theoretically shown that the system can be unstable if the relation of polarities of the two combined piezoelectric elements of a certain vibration mode is different from that of the target vibration mode. Two methods which improve the stability were proposed, and they were applied to the experimental apparatus so as to avoid such instability. It is shown that stress transmission between two combined piezoelectric elements causes the increase of capacitance and the decrease of the performance.

References

(1) R. L. Forward, Electronic damping of vibrations in optical structures, *Applied Optics*, Vol. 18, No. 5 (1979), pp. 690-697.

(2) J. J. Dosch and D. J. Inman, A self-sensing piezoelectric actuator for collocated control, *Journal of Intelligent Material Systems and Structures*, Vol. 3 (1992), pp. 166-185.

(3) K. Yamada, H Matsuhisa, H. Utsuno, and J. G. Park, Passive vibration suppression in flexible structures using piezoelectric elements and LR circuit, *Proceedings of the 11th Asia Pacific Vibration Conference*, (2005), pp. 525-530.

(4) N. W. Hagood and A. V. Flotow, Damping of structural vibrations with piezoelectric materials and passive electrical networks, *Journal of Sound and Vibration*, Vol. 146, No. 2 (1991), pp. 243-268.

(5) C. H. Park and D. J. Inman, A uniform model for series R-L and parallel R-L shunt circuits and power consumption, *Proceedings of SPIE Conference on Smart Structures and Integrated Systems*, Vol. 3668 (1999), pp. 797-804.

(6) S. Y. Wu, Method for multiple mode piezoelectric shunting with single PZT transducer for vibration control, *Journal of Intelligent Material Systems and Structures*, Vol. 9 (1998), pp. 991-998.

(7) G. S. Agnes, Development of a modal model for simultaneous active and passive piezoelectric vibration suppression, *Journal of Intelligent Material Systems and Structures*, Vol. 6 (1995), pp. 482-487.

(8) M. S. Tsai and K. W. Wang, On the structural damping characteristics of active piezoelectric actuators with passive shunt, *Journal of Sound and Vibration*, Vol. 221, No. 1 (1999), pp. 1-22.

(9) K. Adachi, Y. Awakura, and T. Iwatsubo, Hybrid piezoelectric damping for structural vibration suppression, *Journal of Intelligent Material Systems and Structures*, Vol. 15 (2004), pp. 795-801.

(10) J. Ormondroyd and J. P. D. Hartog, The theory of the dynamic vibration absorber, *Transactions of the American Society of Mechanical Engineers*, Vol. 50, No. 7 (1928), pp. 9-22.

(11) K. Yamada, H. Matsuhisa, H. Utsuno, and J. G. Park, Precise measurement technique of the electromechanical coupling coefficient of piezoelectric elements, *Proceedings of the 8th International Conference on Motion and Vibration Control*, (2006), MA1-3.